Contribution of kaon component in viscosity and conductivity of hadronic medium

Mahfuzur Rahaman,[1,2] Snigdha Ghosh,[1,2] Sabyasachi Ghosh,[3,*] Sourav Sarkar,[1,2] and Jan-e Alam[1,2]

[1] Variable Energy Cyclotron Centre 1/AF Bidhannagar, Kolkata 700 064, India
[2] Homi Bhabha National Institute, Training School Complex, Anushaktinagar, Mumbai - 400085, India
[3] Department of Physics, University of Calcutta, 92, A. P. C. Road, Kolkata - 700009, India

With the help of effective Lagrangian densities of strange hadrons, we have calculated kaon relaxation time from several loop and scattering diagrams at tree-level, which basically represent contributions from $1 \leftrightarrow 2$ and $2 \leftrightarrow 2$ type of collisions. Using the total relaxation time of kaon, shear viscosity and electrical conductivity of this kaon component have been estimated. The high temperature, close to transition temperature, where kaon relaxation time is lower than life time of RHIC or LHC matter, may be the only relevant domain for this component to contribute in hadronic dissipation. Our results suggest that kaon can play an important role in the enhancement of shear viscosity and electrical conductivity of hadronic matter near the transition temperature.

PACS numbers:

I. INTRODUCTION

Collisions of heavy ions at highly relativistic energies at the Relativistic Heavy Ion Collider (RHIC) [1–4] and Large Hadron Collider (LHC) [5–7] produce a very hot and dense matter with quarks and gluons as its elementary constituents; this state of matter is known as quark-gluon plasma (QGP). It behaves like a perfect fluid characterized by low shear viscosity to entropy ratio [1–4]. Within the framework of ADS/CFT correspondence [8] Kovtun, Son and Starinets (KSS) [9], conjectured the lowest bound of shear viscosity (η) as, $\eta \geq s/4\pi$, where s is the entropy density. One of the major objectives of these experiments is to understand the quark-hadron transition in the early universe.

In this context it is important to understand how the matter, created in the experiments of heavy ion collision, evolves in space and time. The relativistic viscous hydrodynamics is an efficient tool to simulate this evolution. Various transport coefficients such as shear and bulk viscosities are required as inputs to these simulations in addition to initial conditions and equation of state (EoS). These transport coefficients of quark and hadronic matter can be calculated microscopically by using effective interaction models and this is one of the active fields of contemporary research in heavy ion physics. It is important to investigate the dependence of these transport coefficients on temperature of the medium to characterize the state of the matter. In particular, it is crucial to know the temperature dependence of η/s in order to describe the elliptic flow of hadrons in ultra-relativistic heavy-ion collisions at RHIC and LHC [10, 11].

A lot of work have been done on calculation of the shear viscosity of hadronic matter [12–21]. Some effective QCD model calculations [22–31] gave the estimation of η in both hadronic and quark temperature domain. There are also results, based on numerical simulation, addressed in Refs [32–35].

In this work we also estimate the electrical conductivity σ of the hadronic system which has rich phenomenological and theoretical implications in heavy ion physics. The electrical conductivity can be associated to the rate of soft dilepton production [36] and photon multiplicity near zero transverse momentum [14, 37]. It also controls the rate of decay of the magnetic fields in the system produced in heavy ion collisions [38].

Several authors [24, 37, 39–57] have calculated σ by employing different methods such as - unitarization of chiral perturbation theory [14, 37], numerical solution of Boltzmann transport equation [39, 40], dynamical quasi-particle model [24], off-shell transport model [41, 42], techniques of holography [43], Dyson - Schwinger approach [44] and lattice gauge theory [45–51].

Among the earlier works we find that Refs. [12–21] and Refs. [37, 54–57] deal with shear and electrical conductivity of hadronic matter respectively where majority of these in [12–17, 37, 55–57] considered hadrons in the u, d sector only. Shear viscosity has been estimated by including strangeness in hadron resonance gas (HRG) model in Refs [18–20, 54]. Though some of the effective QCD model calculations, mentioned above, also included strange quark sector but their contribution has not been discussed separately. Since the melting of strange quark condensate is quite different from condensate of u and d quarks, so the contribution of the strange sector in transport coefficients may be necessary to consider separately. This fact may be supported from the recent Ref. [58], where a second peak of bulk viscosity is observed because of the strange quark contribution.

Calculating the relaxation time of kaon, its contribution to shear viscosity of hadronic matter has been discussed in Refs [59, 60]. Here we are interested to focus on this issue with the help of effective hadronic interactions in the strange sector. In Refs. [12, 14, 16, 17, 37, 55, 56], we have seen that effective interactions of pion with σ and ρ resonances are quite successful to describe the (nearly) perfect fluid nature of hadronic matter. In the strange sector, one can use the effective interaction of kaon with

*Electronic address: sabyaphy@gmail.com

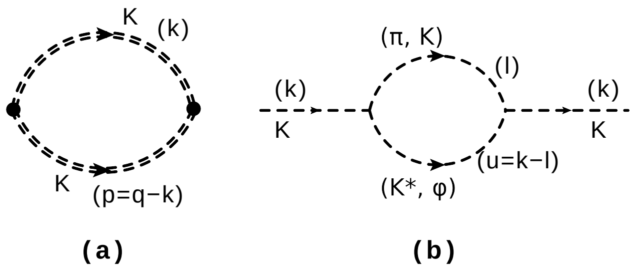

FIG. 1: The diagram (a) is a schematic one-loop representation of viscous-stress tensor for the medium with constituents of K-meson. The double dashed lines for the K-meson propagators indicate that they have some finite thermal width. The diagram (b) is kaon self-energy for πK^* and $K\phi$ loops.

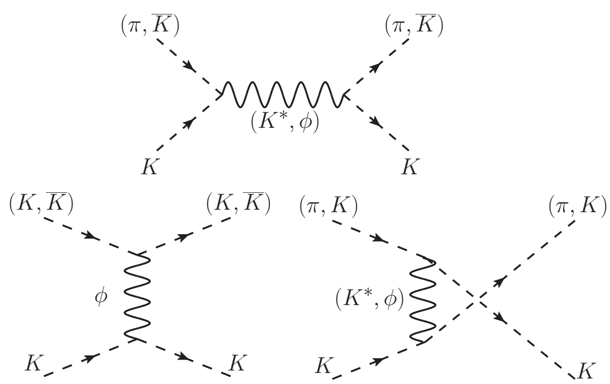

FIG. 2: Tree-level Feynman diagrams of $Kx \to Kx$ scattering, where $x = K, \overline{K}, \pi$.

K^* and ϕ resonances, whose contribution in shear viscosity and electrical conductivity is the aim of present investigation. These transport coefficients are estimated by using their standard expressions, obtained from relaxation time approximation (RTA) or Kubo formalism with one-loop diagram, where the relaxation time or thermal width has been obtained from the effective hadronic Lagrangian density of strange sector.

The paper is organized as follows. In the next section, we have addressed the formalism to calculate the shear viscosity and electrical conductivity of kaon component in term of its thermal width. This section also includes the derivation of kaon thermal width from different possible loop and scattering diagrams. The numerical results on these transport coefficients for kaon component have been discussed in section III. Section IV is devoted to summary and conclusion.

II. FORMALISM

We consider a hot mesonic matter, where pion and kaon are the main constituents of the medium. Here, our main focus is on the constituent of strange sector meson - the kaons. In the next section we derive the expression for viscosity in terms of the width of the kaons in thermal bath.

A. Shear viscosity

We start with the viscous-stress tensor $\pi^{\mu\nu}$ for kaonic medium to construct the spectral density

$$A_K^\eta = \int d^4x e^{iq\cdot x} \langle [\pi_{ij}(x), \pi^{ij}(0)] \rangle_\beta \ , \tag{1}$$

where $\langle \hat{O} \rangle_\beta$ stands for the thermal ensemble average of $\hat{O}$ *i.e.* $\langle \hat{O} \rangle_\beta = \text{Tr}e^{-\beta H}\hat{O}/\text{Tr}e^{-\beta H}$. With the help of the Kubo formalism [61, 62], one can relate this spectral density A_K^η with the shear viscosity (η_K) of kaonic medium as [14]

$$\eta = \frac{1}{20} \lim_{q_0, \mathbf{q} \to 0} \frac{A_K^\eta}{q_0} \ . \tag{2}$$

Following quasi-particle method of Kubo framework [14, 15, 63, 64], the simplest one-loop expressions of Eq. (2) for kaon (K) is:

$$\eta_K = \frac{\beta I_K}{30\pi^2} \int_0^\infty \frac{d\mathbf{k}\mathbf{k}^6}{{\omega_k^K}^2 \Gamma_K} n_k(\omega_k^K)\{1 + n_k(\omega_k^K)\} \ , \tag{3}$$

where isospin factor $I_K = 4$ and $n_k(\omega_k^K) = 1/\{e^{\beta\omega_k^K} - 1\}$ is the Bose-Einstein (BE) distribution of kaon with energy $\omega_k^K = (\mathbf{k}^2 + m_K^2)^{1/2}$. Fig. 1(a) represents the schematic one-loop diagram, derived from two point function of viscous stress tensor in the kaonic medium. Γ_K in Eq. (3) is the thermal width of kaon in the medium which is represented in Fig. 1(a) by double lines. Hence, these internal lines are drawn in double line pattern. This adoption of finite thermal width is a very well established technique [14, 15, 63, 64], which is generally used in Kubo approach to get a non-divergent value of the shear viscous coefficient. This treatment is equivalent to quasi-particle approximation.

Again, this one-loop expression of shear viscosity from Kubo approach [14, 15, 63, 64] exactly coincides with the expression originating from the relaxation-time approximation of the kinetic theory approach [16, 59, 63, 71] Although, RTA is used in the present work for simplicity, we should, however, mention here that the re-summation of ladder diagrams [14, 65–70] leads to the contribution to shear viscosity which has the same order of magnitude as the one loop diagram. The dissipative part of energy momentum tensor, responsible for shear viscosity coefficient, can be expressed as

$$T^{\mu\nu}_D = \eta(D^\mu u^\nu + D^\nu u^\mu + \frac{2}{3}\Delta^{\mu\nu}\partial_\sigma u^\sigma) = \int \frac{d^3\mathbf{k}}{(2\pi)^3}\frac{k^\mu k^\nu}{\omega^K_k}\delta n \ , \quad (4)$$

where

$$D^\mu = \partial^\mu - u^\mu u_\sigma \partial_\sigma, \text{ and } \Delta^{\mu\nu} = u^\mu u^\nu - g^{\mu\nu} \ . \quad (5)$$

It is interesting to note that Eq. (4) relates the collective fluid four velocity, u^μ to the four momentum of elementary constituent, k^μ through the non-equilibrium distribution function $n = n_k + \delta n$, which is assumed to be slightly shifted from equilibrium distribution function n_k by δn, given by

$$\delta n = C k_\mu k_\nu (D^\mu u^\nu + D^\nu u^\mu + \frac{2}{3}\Delta^{\mu\nu}\partial_\sigma u^\sigma) n_k(1+n_k) \ , \quad (6)$$

The Boltzmann equation in RTA can be written as,

$$k^\mu \partial_\mu n_k = \frac{\omega^K_k}{\tau_K}\delta n \ , \quad (7)$$

which fixes the value of C as $C = \frac{\tau_K \beta}{2\omega^K_k}$. Using this expression of C in Eq. (6) one can obtain Eq. (3) through Eq. (4) in RTA approach where we have to identify the kaon relaxation time $\tau_K = 1/\Gamma_K$. Hence, the thermal width or relaxation time of kaon plays a vital role in determining the numerical strength of shear viscosity. To calculate this kaon relaxation time, we have considered two sources of Feynman diagrams. One is loop diagram of kaon self-energy and another is tree-level diagram for elastic scattering channel of kaon. These are described below.

B. Loop diagrams

Following the Cutkosky rule, we will estimate the thermal width from the imaginary part of kaon self-energy at finite temperature. Here, we have considered πK^* and $K\phi$ loops for calculating kaon self-energy, which is shown in Fig. 1(b). We can write the total thermal width/Landau damping (LD) of kaon Γ_K as

$$\Gamma^{LD}_K = -\text{Im}\Pi^{LD}_{K(\pi K^*)}(k_0 = \omega^K_k, \mathbf{k})/(2\omega_K) - \text{Im}\Pi^{LD}_{K(K\phi)}(k_0 = \omega^K_k, \mathbf{k})/(2\omega_K) \ , \quad (8)$$

where $\Pi^{LD}_{K(\pi K^*)}(k)$ and $\Pi^{LD}_{K(K\phi)}(k)$ are kaon self-energy for πK^* and $K\phi$ loops respectively. The subscript, K indicates the external mesons and the mesons within parenthesis stand for those present in the internal lines of the kaon self-energy graphs as shown in Fig. 1(b).

The imaginary part of kaon self-energy for πK^* and $K\phi$ loops are respectively given as:

$$\text{Im}\Pi^{LD}_{K(\pi K^*)}(k) = \int \frac{d^3\mathbf{l}}{32\pi^2 \omega^\pi_l \omega^{K^*}_u} L_{K(\pi K^*)}(k,l)\,|_{l_0=-\omega^\pi_l} \{n_l(\omega^\pi_l) - n_u(\omega^{K^*}_u = k_0 + \omega^\pi_l)\} \delta(k_0 + \omega^\pi_l - \omega^{K^*}_u) \ , \quad (9)$$

and

$$\text{Im}\Pi^{LD}_{K(K\phi)}(k) = \int \frac{d^3\mathbf{l}}{32\pi^2 \omega^K_l \omega^\phi_u} L_{K(K\phi)}(k,l)\,|_{l_0=-\omega^K_l} \{n_l(\omega^K_l) - n_u(\omega^\phi_u = k_0 + \omega^K_l)\} \delta(k_0 + \omega^K_l - \omega^\phi_u) \ , \quad (10)$$

where $n_l(\omega^\pi_l)$, $n_u(\omega^{K^*}_u = k_0 + \omega^\pi_l)$, $n_l(\omega^K_l)$, $n_u(\omega^\phi_u = k_0 + \omega^K_l)$, are BE distribution functions of π, K^*, K and ϕ mesons respectively.

Using the interaction Lagrangian densities [76] :

$$\mathcal{L}^{\text{int}}_{K\pi K^*} = i g_{K\pi K^*}[\overline{K}^{*\mu}\cdot\vec{\tau}\{K(\partial_\mu \pi) - (\partial_\mu K)\pi\}] + h.c. \ , \quad (11)$$

and

$$\mathcal{L}^{\text{int}}_{KK\phi} = g_{KK\phi}[\phi^\mu\{\overline{K}(\partial_\mu K) - (\partial_\mu \overline{K})K\}] \ , \quad (12)$$

we obtain the $K\pi K^*$ and $KK\phi$ vertices as:

$$L(k,l)_{K\pi K^*} = g^2_{K\pi K^*}[\{k^2 + l^2 + 2(k\cdot l)\} - \frac{(k^2 - l^2)^2}{m^2_{K^*}}] \ , \text{ for } \pi K^* \text{ loop} \ , \quad (13)$$

and

$$L(k,l)_{KK\phi} = g^2_{KK\phi}[\{k^2 + l^2 + 2(k\cdot l)\} - \frac{(k^2 - l^2)^2}{m^2_{\phi}}] \ , \text{ for } K\phi \text{ loop} \ . \quad (14)$$

The effective coupling constants $g_{K\pi K^*}/(4\pi) = 0.86$ and $g_{KK\phi}/(4\pi) = 1.82$ are fixed [76] from the experimental decay widths of the processes $K^* \to K\pi$ and $\phi \to K\overline{K}$ respectively.

C. Elastic scattering diagrams

The $2 \leftrightarrow 2$ kind of elastic scattering diagrams, shown in Fig (2), are another possible source along with the LD source, which basically represents $1 \leftrightarrow 2$ type inelastic processes in the medium [72]. The expression of Γ^{Sc}_K for $Kx \to Kx$ scatterings is

$$\Gamma^{Sc}_K = \sum_{x=K,\overline{K},\pi} \int \frac{d^3\mathbf{p}}{(2\pi)^3} v_{Kx}\sigma_{Kx} n^x_p(1 + n^x_p) \ , \quad (15)$$

where relative velocity between K and x meson is given by,

$$v_{Kx} = \frac{[\{s-(m_K+m_x)^2\}\{s-(m_K-m_x)^2\}]^{1/2}}{2\omega_K\omega_x} ,$$
$$\text{with } s = (\omega_K+\omega_x)^2,\ \omega_K = \{\mathbf{k}^2+m_K^2\}^{1/2},$$
$$\omega_x = \{\mathbf{p}^2+m_x^2\}^{1/2}, \tag{16}$$

and $n_p^x = 1/\{e^{\beta\omega_x}-1\}$ is the BE distribution function for x meson. From different possible tree-level elastic scattering diagrams, shown in Fig. (2), the cross section σ_{Kx} of Kx scattering are obtained as

$$\sigma_{Kx} = \frac{1}{16\pi\lambda(s,m_K^2,m_x^2)}\int_{t_{min}}^{t^{max}} |\overline{M_{Kx}}|^2 dt , \tag{17}$$

where $\lambda(s,m_K^2,m_x^2) = s^2+m_K^4+m_x^4-2sm_K^2-2sm_x^2-2m_K^2m_x^2$, known as the Källén function and the limits of the above integration are $t_{max}=0$ and $t_{min}=-\lambda(s,m_K^2,m_x^2)/s$. With the help of the same interaction Lagrangian densities, given in Eqs. (11) and (12), we can construct matrix elements of three different elastic channels - (1). $KK\to KK$, (2). $K\pi\to K\pi$, and (3). $K\overline{K}\to K\overline{K}$, which are respectively written below. The square of the iso-spin averaged amplitude for the elastic scattering of particles, $K(k)$ and $x(p)$ with incident momenta k and p respectively is generically denoted by $|\overline{M_{Kx}}|^2$. The relevant amplitudes are as follows: (1) The square of the iso-spin averaged amplitude for $K(k)K(p)\longrightarrow K(k')K(p')$ is:

$$|\overline{M_{KK}}|^2 = \frac{1}{4}\Big[3|M_{KK}^1|^2+|M_{KK}^0|^2\Big] , \tag{18}$$

where

$$M_{KK}^1 = g_{\phi KK}^2\Big[\frac{(u-s)}{(t-m_\phi^2+i\epsilon)}+\frac{(t-s)}{(u-m_\phi^2+i\epsilon)}\Big] , \tag{19}$$

$$M_{KK}^0 = g_{\phi KK}^2\Big[\frac{(u-s)}{(t-m_\phi^2+i\epsilon)}-\frac{(t-s)}{(u-m_\phi^2+i\epsilon)}\Big] . \tag{20}$$

(2) Amplitude for $K(k)\pi(p)\longrightarrow K(k')\pi(p')$ is,

$$|\overline{M_{K\pi}}|^2 = \frac{1}{3}\Big[2|M_{K\pi}^1|^2+|M_{K\pi}^0|^2\Big] , \tag{21}$$

where

$$M_{K\pi}^{3/2} = 2g_{\pi KK^*}^2\Big[\frac{(t-s)+(m_K^2-m_\pi^2)^2/m_{K^*}^2}{(u-m_{K^*}^2+i\epsilon)}\Big] , \tag{22}$$

$$M_{K\pi}^{1/2} = g_{\pi KK^*}^2\Big[3\{\frac{(t-u)+(m_K^2-m_\pi^2)^2/m_{K^*}^2}{(s-m_{K^*}^2+i\epsilon)}\} -\{\frac{(t-s)+(m_K^2-m_\pi^2)^2/m_{K^*}^2}{(u-m_{K^*}^2+i\epsilon)}\}\Big] . \tag{23}$$

(3) Similarly for the process, $K(k)\overline{K}(p)\longrightarrow K(k')\overline{K}(p')$ the amplitude is:

$$|\overline{M_{K\overline{K}}}|^2 = \frac{1}{4}\Big[3|M_{K\overline{K}}^1|^2+|M_{K\overline{K}}^0|^2\Big] , \tag{24}$$

where

$$M_{K\overline{K}}^1 = g_{\phi KK}^2\Big[\frac{s-u}{t-m_\phi^2+i\epsilon}\Big] , \tag{25}$$

$$M_{K\overline{K}}^0 = g_{\phi KK}^2\Big[\frac{2(t-u)}{(s-m_\phi^2+i\epsilon)}+\frac{(s-u)}{(t-m_\phi^2+i\epsilon)}\Big] . \tag{26}$$

In the above expressions, the Mandelstam variables are $s=(k+p)^2$, $t=(k-k')^2$, $u=(k'-p)^2$. We have also taken the experimental values of decay widths for K^* and ϕ mesons propagators in s-channel diagrams of Fig. (2).

D. Nucleonic matter

Now we would like to estimate the effects of kaon-nucleon interaction on the width of kaons in the thermal bath. For this purpose the natural way to proceed is to calculate the possible baryon loops contributing to the kaon self-energy. The $N\Lambda$ and $N\Sigma$ can be considered as possible candidates. The Landau and unitary cut contributions to kaon self-energy can be calculated using effective $KN\Lambda$ and $KN\Sigma$ interaction Lagrangian densities. However, we do not get any on-shell value for kaon relaxation time because kaon pole (m_k) is located neither in its Landau cut region (0 to $|m_{\Lambda,\Sigma}-m_N|$) nor in its unitary cut region ($|m_{\Lambda,\Sigma}+m_N|$ to ∞), where $m_N=0.940$ GeV, $m_\Lambda=1.115$ GeV and $m_\Sigma=1.189$ GeV are the masses of N, Λ and Σ baryons respectively. Therefore, instead of this methodology of loop calculation, we have resorted to the following alternative way.

Let us take the experimental values of scattering length a_{KN}^I of KN interaction, where I stands for different isospin states of KN system. From Refs. [73–75], using the scattering lengths $a_{KN}^{I=0}=-0.007$ fm and $a_{KN}^{I=1}=-0.225$ fm, we obtain the isospin averaged cross section,

$$\sigma_{KN} = 4\pi\sum_{I=0,1}(2I+1)|a_{KN}^I|^2\Big/\sum_{I=0,1}(2I+1) \approx\ 4.7\text{ mb} , \tag{27}$$

which can be used to calculate the relaxation time τ_{KN} or thermal width Γ_{KN} of K by using Eq. (15), where x meson is replaced by nucleon N and its distribution function will be (Fermi-Dirac) $n_p^N = 1/\{e^{\beta\omega_N}+1\}$.

Finally, for total thermal width of K, we have to add LD and scattering part of mesonic matter, described in subsection (II B), (II C) and the nucleonic matter contribution, described in subsection (II D). We however find that the nucleonic matter has negligibly small numerical contribution.

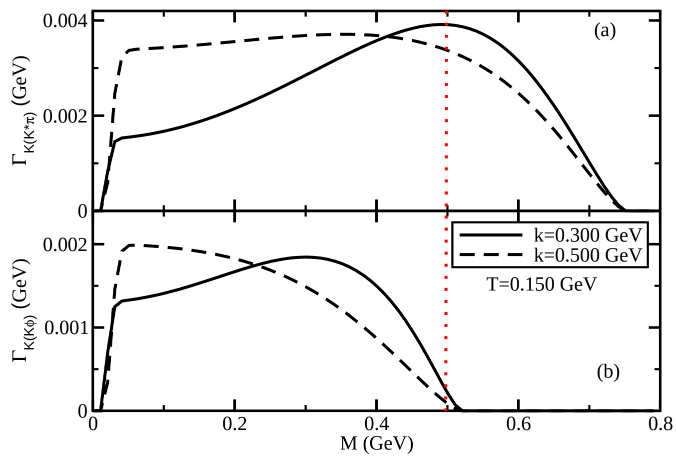

FIG. 3: (Color online) The thermal width of kaon self-energy from (a)$K^*\phi$ and (b) $K\phi$ loops as a function of invariant mass $M=\sqrt{k_0^2-|\mathbf{k}|^2}$ at fixed temperature $T=0.150$ GeV for two different momenta $\mathbf{k}=0.300$ GeV (solid line) and 0.500 GeV (dashed line). The vertical red dotted line represents the on-shell value $M=m_K$.

E. Electrical conductivity

Similar to shear viscosity, one can derive the expression for electrical conductivity, σ_K for kaon component, using the spectral density of current-current correlator

$$A_K^\sigma=\int d^4x e^{iq\cdot x}\langle[J_i(x),J^i(0)]\rangle_\beta\ . \tag{28}$$

The corresponding Kubo relation reads,

$$\sigma_K=\frac{1}{6}\lim_{q_0,\mathbf{q}\to 0}\frac{A_K^\sigma}{q_0}\ . \tag{29}$$

Within the one loop approximation the expression for σ_K is given by [37, 55]

$$\sigma_K=\frac{g_K^e}{3T}\int\frac{d^3\mathbf{k}}{(2\pi)^3\Gamma_K}\left(\frac{\mathbf{k}}{\omega_K^k}\right)^2\left[n_K(\omega_K^k)\{1+n_K(\omega_K^k)\}\right]\ , \tag{30}$$

where $g_K^e=2e^2$ is isospin factor for charged kaon - K^+ and K^-. Same expression for σ_K can be obtained in RTA approach.

III. RESULTS AND DISCUSSION

First we explore the contribution of loop diagram in kaon relaxation time. From Eqs. (9) and (10), one can respectively obtain the individual contributions from $K^*\pi$ and $K\phi$ loops to the (off-shell) thermal width of kaon as a function of the invariant mass $M=\sqrt{k_0^2-|\mathbf{k}|^2}$ for two different values of three momenta $\mathbf{k}=0.300$ GeV and $\mathbf{k}=0.500$ GeV at temperature $T=0.150$ GeV. The results are shown in Fig. (3), where we have used

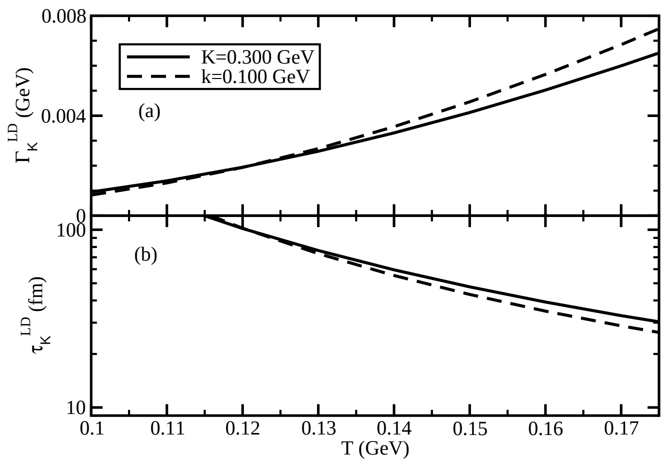

FIG. 4: Temperature dependence of (a) thermal width and (b) the mean free path of kaon for two different momenta $\mathbf{k}$=0.100 GeV (solid line) and $\mathbf{k}$=0.300 GeV (dashed line). The horizontal dashed red line represents an approximate dimension of fireball.

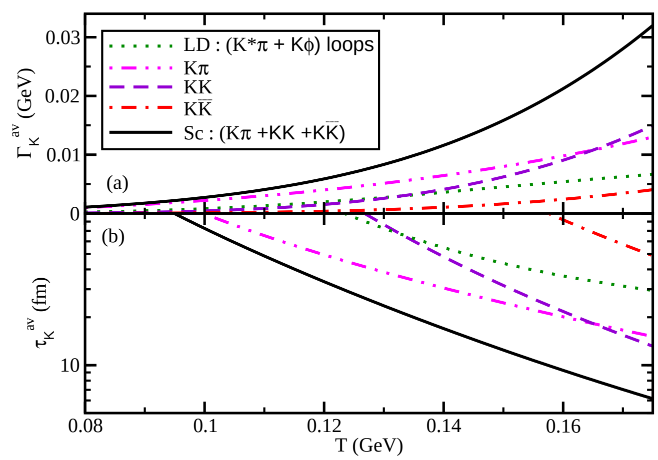

FIG. 5: (Color online) T dependence of average thermal widths (a) and relaxation times (b) for KK (dashed line), $K\pi$ (dash-double-dotted line), $K\overline{K}$ (dash-dotted line) scatterings and their total (solid line) and Landau damping part (dotted line).

$m_\pi=0.140$ GeV, $m_K=0.500$ GeV, m_{K^*}=0.890 GeV, $m_\phi=1.020$ GeV. It is clear that the Landau cuts [17, 72] end sharply at $M=|m_\phi-m_K|=0.51$ GeV for the $K\phi$ loop and $M=|m_{K^*}-m_\pi|=0.745$ GeV for $K^*\pi$ loop. The red vertical dashed line in Fig. (3) denotes the physical pole mass of kaon and its corresponding contribution will provide on-shell values of kaon thermal widths for $K^*\pi$ and $K\phi$ loops respectively. One should keep in mind that these Landau cut contributions only originate in the presence of medium. In vacuum, we can not have any (on-shell) decay like $K\to K^*\pi$ or $K\to K\phi$ because of kinematic restrictions. Here we get a non-zero thermal width of kaon because of in-medium $KK^*\pi$ and

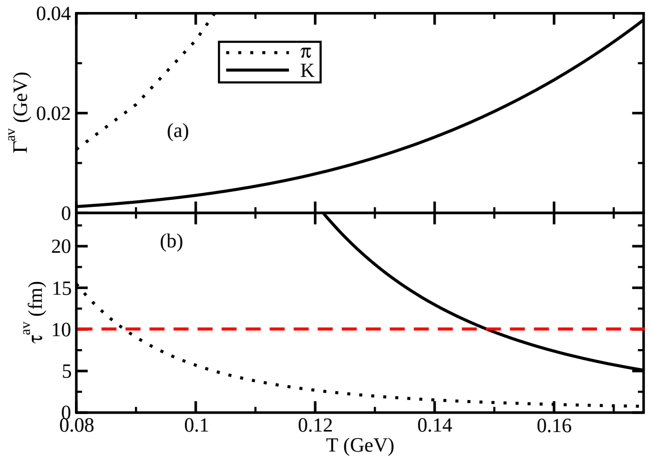

FIG. 6: (Color online) Temperature dependence of average (a) thermal widths and (b) relaxation times of pion (dotted lines) and kaon (solid lines) The horizontal dashed line represents an approximate life time of fireball.

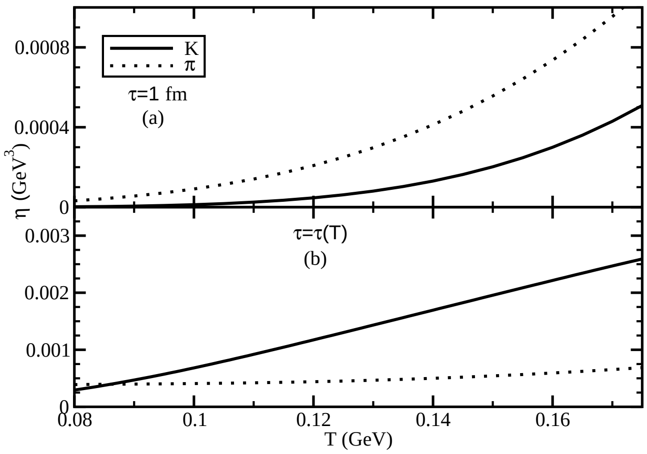

FIG. 7: Temperature dependence of shear viscosity for kaon (solid line) and pion (dotted line) by using (a) $\tau = 1$ fm and (b) $\tau = \tau(T)$.

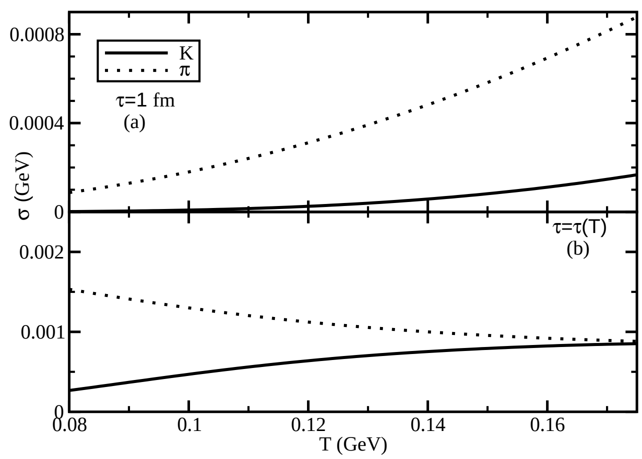

FIG. 8: Same as Fig. 7 for electrical conductivity.

$KK\phi$ scatterings which were absent in vacuum.

In Fig. 4 we display the temperature dependence of total (on-shell) thermal width Γ_K^{LD} and relaxation time $\tau_K^{LD} = 1/\Gamma_K^{LD}$ of kaon for $\mathbf{k} = 0.100$ GeV (solid line) and $\mathbf{k} = 0.300$ GeV (dashed line). The total (on-shell) thermal width of kaon is the summation of $K^*\pi$ and $K\phi$ loop contributions. We observe that the contributions from the former dominates over the latter as revealed in Fig. (3). We observe that the thermal width increases with the temperature. As relaxation time $\tau_K^{\rm LD}$ is inversely proportional to the thermal width (Γ_K), the τ_K^{LD} decreases rapidly as temperature increases. We have seen that the nucleonic contribution due to KN interaction to the kaon thermal width or mean free path is insignificant compared to the contributions from mesonic loops, therefore, the nucleonic part has not been shown separately.

We can take thermal average of $\Gamma_K^{LD}(\mathbf{k}, T)$ by using the relation

$$\Gamma_K^{\rm av} = \int_0^\infty \frac{d^3\mathbf{k}}{(2\pi)^3}\Gamma_K^{LD}(\mathbf{k},T)n_k^K(\omega_k^K)\Big/\int_0^\infty \frac{d^3\mathbf{k}}{(2\pi)^3}n_k^K(\omega_k^K)\,, \tag{31}$$

which is plotted using dashed line in Fig. 5(a). Similar to LD source, different scattering contributions for $K\pi$, KK, $K\overline{K}$ interactions and their total are shown by dash-double-dotted, dashed, dash-dotted and solid lines in Fig. 5(a). Their corresponding relaxation times are drawn in Fig. 5(b). Here we notice that the contribution of elastic scattering is dominating over the LD contribution. After adding them we get total thermal width of kaon, which is plotted by solid line in Fig. 6(a) and it is also compared with the thermal width of pion component (dotted line), taken from Ref. [17]. In Fig. 6(b), their relaxation times are also compared and we noticed that the relaxation time of kaon is greater than that of pion. We consider that the lifetime of fireball produced in heavy ion experiments is approximately 10 fm as indicated by a horizontal (red) dashed line in Fig. 6(b). We observe that the relaxation time induced by the interactions involving pions is smaller than that involving kaons. The life time of the fireball is larger than the pions for almost the entire range of temperature considered. However, the kaons has the chance of getting equilibrated only at high temperatures, $T \sim 150$ MeV which is close to the quark-hadron transition temperature.

In Fig. 7, we present the temperature dependence of shear viscosity of kaon (solid lines) and compare with pion (dotted lines) for (a) constant relaxation times and (b) temperature dependent relaxation times (displayed in Fig. 6). For constant relaxation time, shear viscosity for kaon component is smaller than that of pion but for temperature dependent relaxation time the trend is reversed.

Eq. 3 indicates that for a constant relaxation time (or thermal width) the temperature dependence of shear viscosity is governed by the thermal phase space factors. The massive kaons are thermally more suppressed than the lighter pions in the bath, consequently the η for kaons is smaller than that of pions for the same value of relaxation time ($\tau = 1$ fm/c). This is reflected through the results displayed in the upper panel of Fig. 7.

The shear viscosity represents fluid resistance to the transfer of momentum through collision processes. The momentum transfer gets easier and hence the fluid resistance or the shear viscosity becomes smaller in a strongly interacting medium. Therefore, the inclusion of interactions of pions and kaons in evaluating their shear viscosities is essential. We note that thermal width (the interaction rate) of kaons is smaller than pions since the interaction of kaons is weaker. We find that the viscosity of kaons is larger than the pions because the thermal suppression of kaons is overwhelmed by their larger relaxation time (smaller thermal width) as compared to pions. In other words the smaller relaxation time of pions compensate the larger thermal abundance and hence results in smaller viscosity. In the context of finite size RHIC or LHC matter the kaon component becomes relevant at high T because the kaon relaxation time at $T>$150 MeV is smaller than than the typical fireball life time. Hence, the role of kaon viscosity near the transition temperature cannot be ignored. Similar observation was made in earlier investigations [59, 60] too.

Next, in Fig. 8(a), the temperature dependence of electrical conductivities for kaon (solid lines) and pion (dotted line) are drawn for constant relaxation time τ and similar to Fig. 7(a), pion component is larger than kaon component due to the reason explained above - the massive kaons are thermally suppressed more than pions.

We find that with the temperature dependent thermal width (or relaxation time) the electrical conductivity of pion decreases unlike the shear viscosity which shows a mildly increasing trend with increase in temperature (Fig. 7 b). This difference originates from the expressions of σ and η, given by Eqs. (30) and (3) respectively involving different power of momentum in their integrand. This can be understood easily at the high temperature limit ($T >> m_\pi$) where the electrical conductivity of pions, $\sigma_\pi^{el} \sim T^2/\Gamma^{av}(T)$ and the shear viscosity, $\eta_\pi \sim T^4/\Gamma^{av}(T)$ which clearly indicates that σ_π^{el} and η_π have different T dependence. For the kaon component, both $\eta_K(T)$ and $\sigma_K(T)$ are increasing functions but their slopes are different because of the different exponent of momentum appearing in the expressions for viscosity and electrical conductivity. It is also interesting to note that the pion and kaon contributions to the electrical conductivity is comparable at high T and the nature of T variation will be governed by their combined strengths.

IV. SUMMARY AND CONCLUSION

In this work we have estimated the contributions of strange hadrons to shear viscosity and electrical conductivity of hadronic matter. It is well known that the standard expressions of these transport coefficients can be obtained either from RTA or Kubo framework, where the relaxation time of medium constituents proportionally controls their numerical strengths. We have calculated kaon relaxation time by considering different possible $1 \leftrightarrow 2$ and $2 \leftrightarrow 2$ processes. Contributions from $1 \leftrightarrow 2$ have been calculated from the imaginary part of kaon self-energy at finite temperature. For the calculation of self energy πK^* and $K\phi$ have been considered in the internal lines. For $2 \leftrightarrow 2$ type of elastic channels, $K\pi$, KK and $K\overline{K}$ processes have been considered. All these in-elastic and elastic channels are calculated from an effective hadronic Lagrangian density, describing $KK\phi$ and $KK^*\pi$ interactions. We notice that $2 \leftrightarrow 2$ scattering processes in medium dominate over the $1 \leftrightarrow 2$ processes. The inverse of the total scattering probability, quantified by total thermal width, basically gives the relaxation time of kaons in the medium. If we consider the life time of the hadronic fireball produced at RHIC and LHC collisions ~ 10 fm/c then we notice that the kaon has the chance to attain equilibrium at the high temperature domain close to the transition temperature. It signifies that for phenomenological purpose, the contribution of kaon component is relevant in the high temperature region.

Using the total kaon relaxation time, we have estimated shear viscosity and electrical conductivity of kaon component. When we compare with the pion component, estimated in earlier work [17] using a similar type of effective hadronic interactions, we notice that kaon has smaller electrical conductivity than pions but an opposite trend is observed in shear viscosity *i.e.* the viscosity of kaons is larger than pions. We also note that with the inclusion of $K-\pi$ interaction the magnitude of η_K reduces compared to the scenario when $K-\pi$ interaction is ignored in estimating η_K. However, the inequality, $\eta_K > \eta_\pi$ is still maintained with $K-\pi$ interaction for almost the entire temperature range considered here (η_π is shear viscosity of pion). That is the gap between the η_K and η_π decreases with the introduction of $K-\pi$ interaction but the η_K remains higher in magnitude than η_π as the case when the $K-\pi$ interaction is neglected.

In the context of phenomenological direction, the contribution of kaon component at high temperature may only be relevant and our studies show that kaons play a crucial role in both electrical conductivity and shear viscosity (and possible for other transport coefficients as well) at that high temperature region.

Acknowledgment : Sabyasachi Ghosh is supported from UGC Dr. D. S. Kothari Post Doctoral Fellowship under grant No. F.4-2/2006 (BSR)/PH/15-16/0060. Snigdha Ghosh (CNT project No. 3/2/3012/VECC/R&D-I/1928) and MR are grateful to Department of Atomic Energy, Govt of India for financial support.

---

[1] BRAHMS Collaboration (I. Arsene et al.), Nucl. Phys. **A 757**, 1 (2005)
[2] PHENIX Collaboration (K. Adcox et al.), Nucl. Phys. **A 757**, 184 (2005).
[3] PHOBOS Collaboration (B.B. Back et al.), Nucl. Phys. **A 757**, 28 (2005).
[4] STAR Collaboration (J. Adams et al.), Nucl. Phys. **A 757**, 102 (2005).
[5] ALICE Collaboration (K. Aamodt et al.), Phys. Rev. Lett. **108**, 252302 (2010).
[6] ALICE Collaboration (K. Aamodt et al.), Phys. Lett. **B 696**, 30 (2011).
[7] ALICE Collaboration (D. Caffarri et al.), Nucl. Phys. **A 904-905**, 643c (2013).
[8] G. Policastro, D. T. Son, and A. O. Starinets, Phys. Rev.Lett. **87**, 081601 (2001).
[9] P. Kovtun, D. T. Son, and A. O. Starinets, Phys. Rev. Lett. **94**, 111601 (2005).
[10] H. Niemi, G. S. Denicol, P. Huovinen, E. Molnár, and D. H. Rischke, Phys. Rev. **C 86**, 014909.
[11] D.H. Rischke, Phys. Rev. Lett. **106**, 212302 (2011).
[12] K. Itakura, O. Morimatsu, and H. Otomo, Phys. Rev. **D 77**, 014014 (2008).
[13] A. Dobado and S.N. Santalla, Phys. Rev. **D 65**, 096011 (2002); A. Dobado and F. J. Llanes-Estrada, Phys. Rev. **D 69**, 116004 (2004).
[14] D. Fernandez-Fraile and A. Gomez Nicola, Eur. Phys. J. **C 62**, 37 (2009).
[15] R. Lang, N. Kaiser and W. Weise Eur. Phys. J. **A 48**, 109 (2012).
[16] S. Mitra, S. Ghosh, and S. Sarkar Phys. Rev. **C 85**, 064917 (2012).
[17] S. Ghosh, G. Krein, S. Sarkar, Phys. Rev. **C 89**, 045201 (2014); S. Ghosh, Phys. Rev. **C 90** 025202 (2014); S. Ghosh, Braz. J. Phys. 45 (2015) 687.
[18] M. I. Gorenstein, M. Hauer, O. N. Moroz, Phys. Rev. **C 77**, 024911 (2008).
[19] G. P. Kadam and H. Mishra, Nucl. Phys. **A 934**, 133 (2015); Phys. Rev. C 92, 035203 (2015).
[20] J.Noronha-Hostler, J. Noronha, C. Greiner, Phys. Rev. Lett. **103**, 172302 (2009).
[21] A.S. Khvorostukhin V.D. Toneev a,c , D.N. Voskresensky Nucl. Phys. A 845 (2010)
[22] P. Chakraborty and J. I. Kapusta, Phys. Rev. C **83**, 014906 (2011).
[23] C. Sasaki, K. Redlich, Nucl. Phys. **A 832** (2010) 62.
[24] R. Marty, E. Bratkovskaya, W. Cassing, J. Aichelin, and H. Berrehrah, Phys. Rev. **C 88**, 045204 (2013).
[25] S. Ghosh, A. Lahiri, S. Majumder, R. Ray, S. K. Ghosh, Phys. Rev. **C 88** (2013) 068201.
[26] R. Lang, W. Weise Eur. Phys. J. **A 50**, 63 (2014); R. Lang, N. Kaiser, W. Weise, Eur. Phys. J. **A 51**, 127 (2015).
[27] S. K. Ghosh, S. Raha, R. Ray, K. Saha, S. Upadhaya, Phys. Rev. **D 91**, 054005 (2015).
[28] S. Ghosh, T. C. Peixoto, V. Roy, F. E. Serna, and G. Krein, Phys. Rev. **C 93**, 045205 (2016).
[29] P. Deb, G. Kadam, H. Mishra, Phys. Rev. **D 94** (2016), 094002.
[30] A. N. Tawfik, A. M. Diab, M.T. Hussein, Int. J. Mod. Phys. **A 31** (2016) 1650175.
[31] A. Abhishek, H. Mishra, S. Ghosh, arXiv:1709.08013 [hep-ph]; P. Singha, A. Abhishek, G. Kadam, S. Ghosh, H. Mishra, arXiv:1705.03084 [nucl-th].
[32] N. Demir and S.A. Bass Phys. Rev. Lett. **102**, 172302 (2009).
[33] A. Muronga, Phys. Rev. **C 69**, 044901 (2004).
[34] S. Plumari, A. Puglisi, F. Scardina, and V. Greco, Phys. Rev. **C 86**, 054902 (2012).
[35] S. Pal, Phys. Lett. **B 684** (2010) 211.
[36] G. D. Moore and J. M. Robert, hep-ph/0607172 (2006), arXiv:0607172v1.
[37] D. Fernandez-Fraile and A. Gomez Nicola, Phys. Rev. **D 73**, 045025 (2006).
[38] K. Tuchin, Adv. High Energy Phys. **2013**, 490495 (2013)
[39] A. Puglisi, S. Plumari, V. Greco, Phys. Rev. **D 90**, 114009 (2014); J. Phys. Conf. Ser. 612 (2015) 012057; Phys. Lett. **B 751** (2015) 326.
[40] M. Greif, I. Bouras, Z. Xu, C. Greiner, Phys. Rev. **D 90** (2014) 094014; J. Phys. Conf. Ser. 612 (2015) 012056.
[41] W. Cassing, O. Linnyk, T. Steinert, and V. Ozvenchuk, Phys. Rev. Lett. **110**, 182301 (2013).
[42] T. Steinert and W. Cassing, Phys. Rev. **C 89**, 035203 (2014).
[43] S. I. Finazzo and J. Noronha, Phys. Rev. **D 89**, 106008 (2014).
[44] S.-X. Qin, Phys. Lett. **B 742**, 358 (2015), arXiv:1307.4587.
[45] H.T. Ding, A. Francis, O. Kaczmarek, F. Karsch, E. Laermann, and W. Soeldner, Phys. Rev. **D 83**, 034504 (2011).
[46] G. Aarts, C. Allton, J. Foley, S. Hands, and S. Kim, Phys. Rev. Lett. **99**, 022002 (2007).
[47] P. V. Buividovich, M. N. Chernodub, D. E. Kharzeev, T. Kalaydzhyan, E. V. Luschevskaya, and M. I. Polikarpov, Phys. Rev. Lett. **105**, 132001 (2010).
[48] Y. Burnier and M. Laine, Eur. Phys. J. **C 72**, 1902 (2012).
[49] S. Gupta, Phys. Lett. **B 597**, 57 (2004).
[50] B. B. Brandt, A. Francis, H. B. Meyer, and H. Wittig, J. High Energy Phys. **03** (2013) 100.
[51] A. Amato, G. Aarts, C. Allton, P. Giudice, S. Hands, J.I. Skullerud, Phys. Rev. Lett. **111**, 172001 (2013).
[52] P. K. Srivastava, L. Thakur, B. K. Patra, Phys. Rev. **C 91**, 044903 (2015).
[53] S. Ghosh, F. E. Serna, A. Abhishek, G. Krein, H. Mishra *in progress*
[54] M. Greif, C. Greiner, G.S. Denicol, Phys. Rev. **D 93**, 096012 (2016).
[55] S. Ghosh, Phys. Rev. **D 95**, 036018 (2017).
[56] S. Ghosh, S. Mitra, S. Sarkar Nucl. Phys. A969 (2018) 237.
[57] C. Lee, I. Zahed, Phys. Rev. **C 90**, 025204 (2014).
[58] K. Saha, S. Ghosh, S. Upadhaya, S. Maity, arXiv:1711.10169 [nucl-th].
[59] M. Prakash, M. Prakash, R. Venugopalan, and G. Welke,

Phys. Rep. **227**, 321 (1993).

[60] J. I. Kapusta, "Viscous Properties of Strongly Interacting Matter at High Temperature,"*Relativistic Nuclear Collisions*, Landolt-Bornstein New Series, Vol. I/23, ed. R. Stock (Springer-Verlag, Berlin Heidelberg 2010);arXiv:0809.3746 [nucl-th].

[61] D. N. Zubarev *Non-equilibrium statistical thermodynamics* (New York, Consultants Bureau, 1974).

[62] R. Kubo, J. Phys. Soc. Jpn. **12**, 570 (1957).

[63] S. Mallik and S. Sarkar, Hadrons at Finite Temperature, Cambridgee University Press, 2016.

[64] S. Ghosh, Int. J. Mod. Phys. **A 29** (2014) 1450054.

[65] S. Jeon, Phys. Rev. **D 52** (1995) 3591.

[66] S. Jeon, L. G. Yaffe, Phys. Rev. **D 53** (1996) 5799.

[67] A. Czajka, S. Jeon, Phys. Rev. **C 95**, 064906 (2017).

[68] P. Arnold, G.D. Moore, L.G. Yaffe, JHEP 0011 (2000) 001.

[69] P. Arnold, G.D. Moore, L.G. Yaffe, JHEP 0305 (2003) 051.

[70] P. Arnold, C. Dogan, G. D. Moore, Phys. Rev. **D 74**, 085021 (2006).

[71] S. Gavin, Nucl. Phys. **A, 435**, 826 (1985).

[72] H.A. Weldon, Phys. Rev. **D 28**, 2007 (1983).

[73] M. Fukugita, Y. Kuramashi, M. Okawa, H. Mino, A. Ukawa, Phys. Rev. **D 52**, 3003 (1995).

[74] M. M. Nagels et al. , Nucl. Phys. **B 147**, 189 (1979)

[75] O. Dumbrajs et al. , Nucl. Phys. **B 216**, 277 (1983).

[76] C.M. Ko, D. Seibert, Phys. Rev. **C 49**, 2198 (1994).